Science Advances
AAAS

advances.sciencemag.org/cgi/content/full/6/47/eabb1981/DC1

Supplementary Materials for

Biophysical impacts of Earth greening largely controlled by aerodynamic resistance

Chi Chen*, Dan Li*, Yue Li, Shilong Piao, Xuhui Wang, Maoyi Huang,
Pierre Gentine, Ramakrishna R. Nemani, Ranga B. Myneni

*Corresponding author. Email: lidan@bu.edu (D.L.); chenchi@bu.edu (C.C.)

Published 20 November 2020, *Sci. Adv.* **6**, eabb1981 (2020)
DOI: 10.1126/sciadv.abb1981

This PDF file includes:

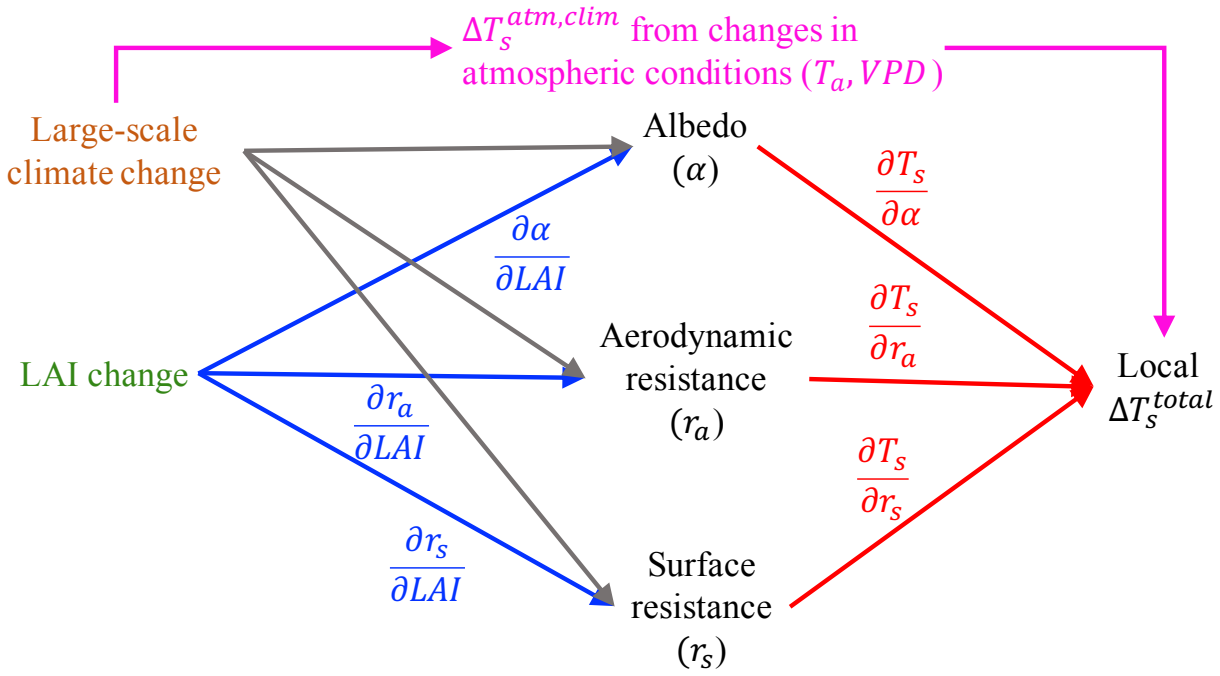

Fig. S1. Schematic diagram of mechanisms affecting LST. The paths in blue arrows will lead to LST change through biophysical factors due to LAI change, $\Delta T_s^{bio,LAI}$; the paths in grey arrows will lead to LST change through biophysical factors due to large-scale climate change, $\Delta T_s^{bio,clim}$, and the paths in pink arrows will lead to LST change through atmospheric conditions due to large-scale climate change, $\Delta T_s^{atm,clim}$.

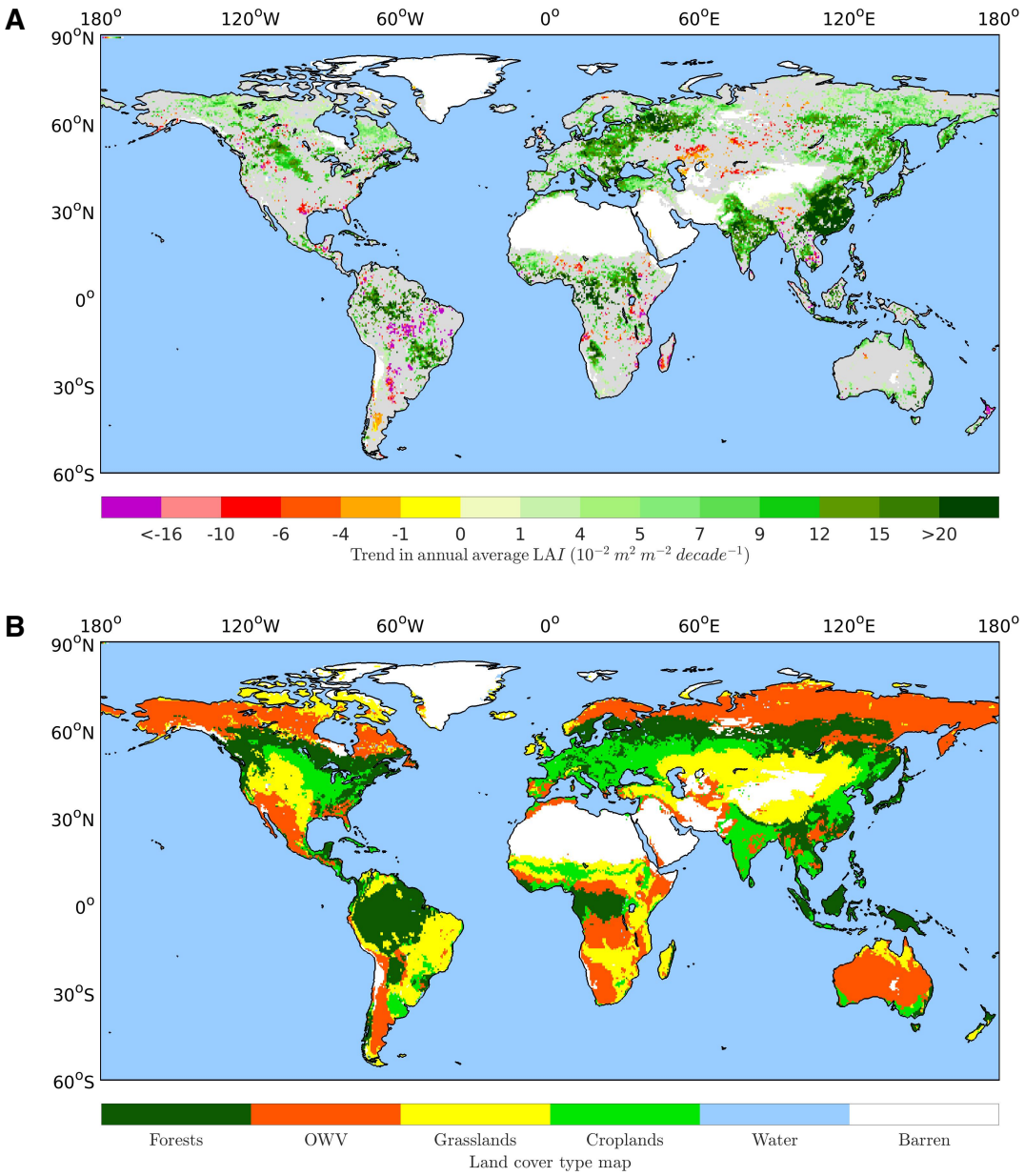

Fig. S2. Maps of broad vegetation classes and trend in MODIS annual average LAI. (**A**) Map of trends in annual average MODIS LAI from 2000 to 2014. Statistically significant trends (Mann–Kendall test, $P \leq 0.1$) are color-coded. Grey areas show vegetated land with statistically insignificant trends. White areas depict barren lands, permanent ice-covered areas, permanent wetlands and built-up areas. Blue areas represent water. (**B**) Map of broad vegetation classes used in the presented analysis. Forests consist of evergreen needleleaf forest, evergreen broadleaf forest,

deciduous needleleaf forest, deciduous broadleaf forest, and mixed forest. Other woody vegetation (OWV) refers to closed shrublands, open shrublands, and woody savannas. Grasslands include savannas and grasslands. Croplands consist of croplands and croplands/natural vegetation mosaic. All aggregations are based on MODIS IGBP classification scheme.

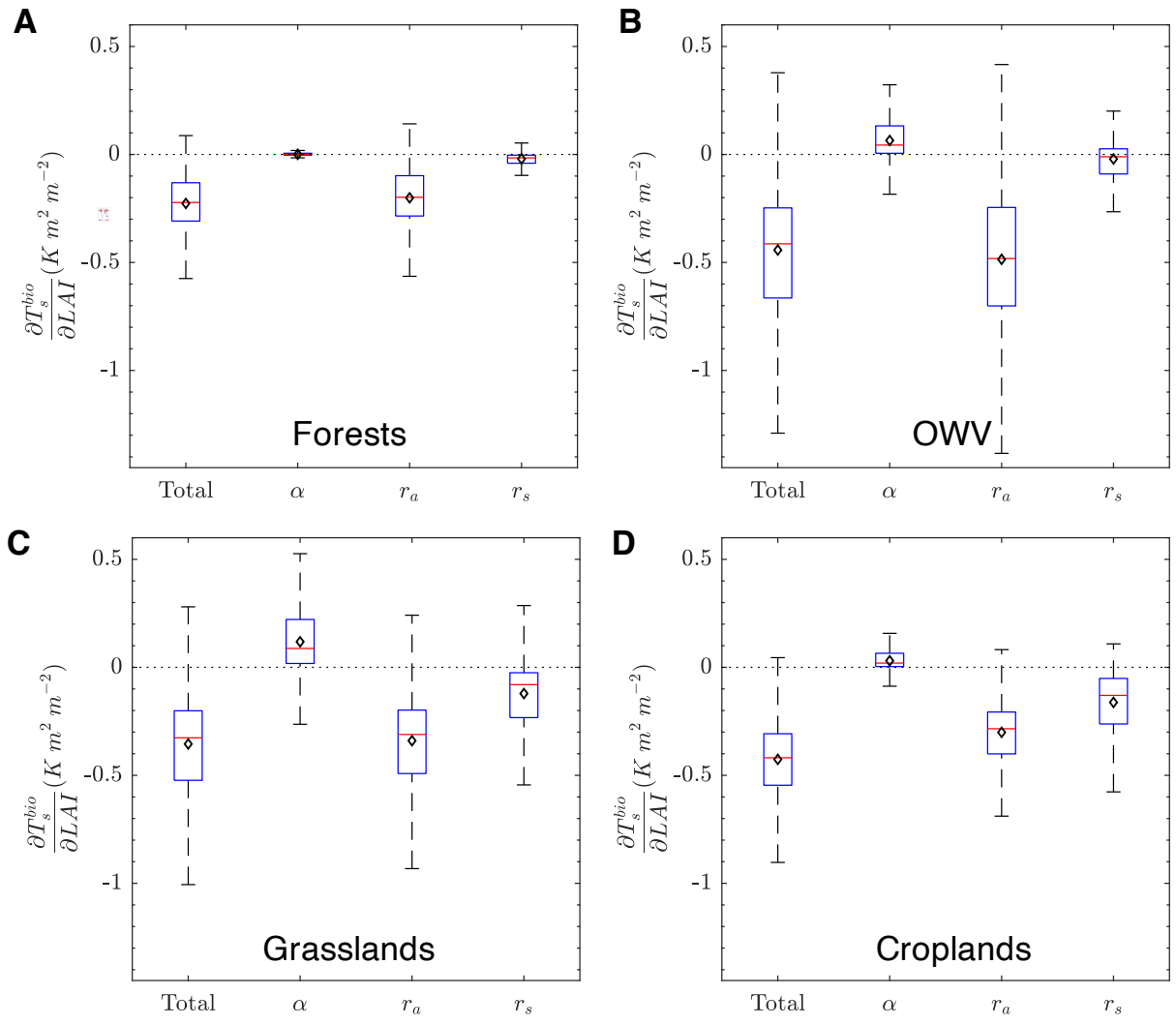

Fig. S3. Attribution of $\frac{\partial T_s^{bio}}{\partial LAI}$ with surface biophysical factors for each biome type. (**A**) Forests. (**B**) Other woody vegetation (OWV). (**C**) Grasslands. (**D**) Croplands. Results are diagnosed from CLM5 outputs using the TRM method presented in boxplot. The diamonds indicate the mean.

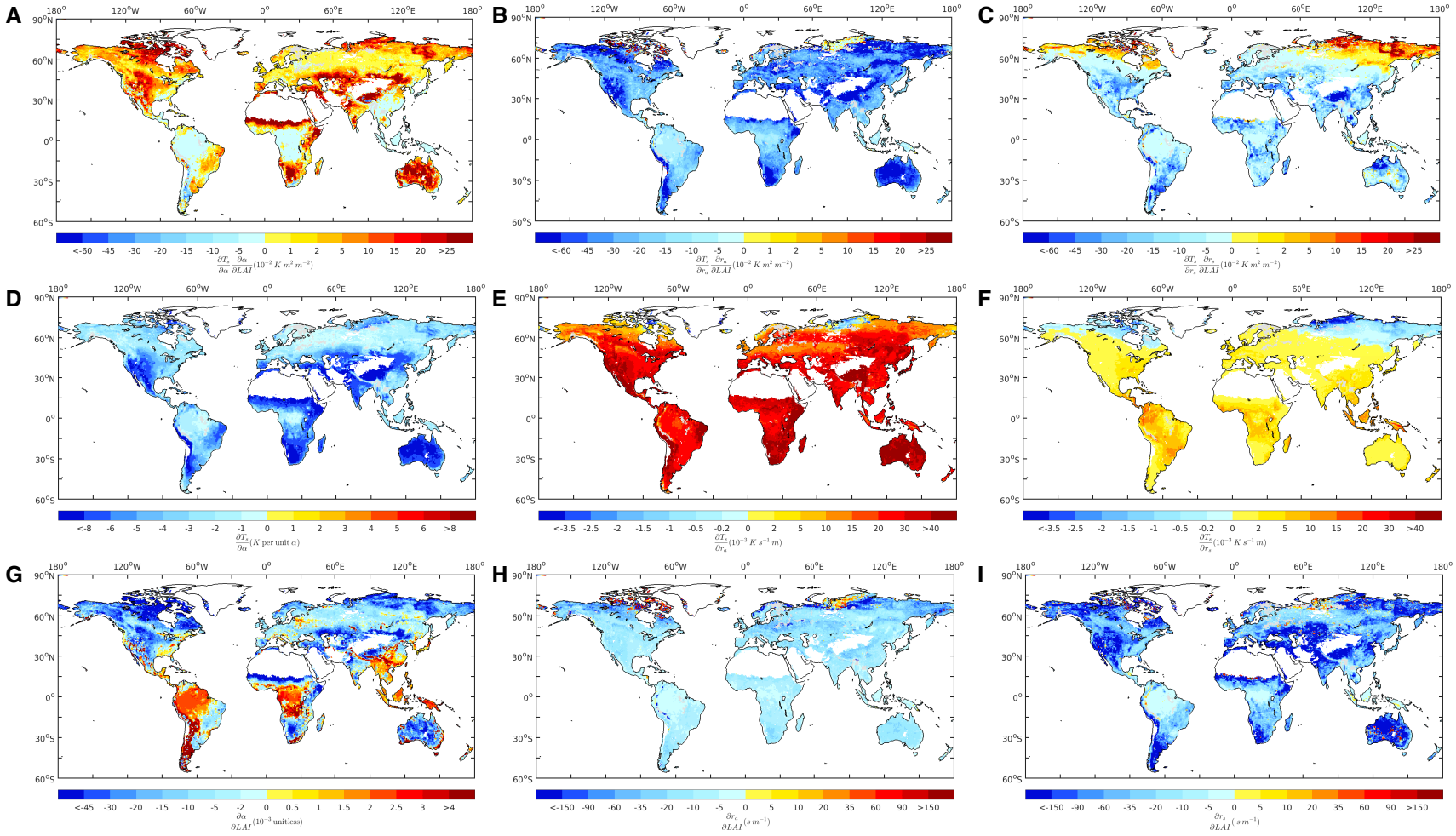
A
B
C
D
E
F
G
H
I
180° 120°W 60°W 0° 60°E 120°E 180°
90°N 60°N 30°N 0° 30°S 60°S
<-60 -45 -30 -20 -15 -10 -5 0 1 2 5 10 15 20 >25
$\frac{\partial T_s}{\partial \alpha}\frac{\partial \alpha}{\partial LAI}(10^{-2}\,K\,m^2\,m^{-2})$
$\frac{\partial T_s}{\partial r_a}\frac{\partial r_a}{\partial LAI}(10^{-2}\,K\,m^2\,m^{-2})$
$\frac{\partial T_s}{\partial r_s}\frac{\partial r_s}{\partial LAI}(10^{-2}\,K\,m^2\,m^{-2})$
<-8 -6 -5 -4 -3 -2 -1 0 1 2 3 4 5 6 >8
$\frac{\partial T_s}{\partial \alpha}(K \text{ per unit } \alpha)$
<-3.5 -2.5 -2 -1.5 -1 -0.5 -0.2 0 2 5 10 15 20 30 >40
$\frac{\partial T_s}{\partial r_a}(10^{-3}\,K\,s^{-1}\,m)$
$\frac{\partial T_s}{\partial r_s}(10^{-3}\,K\,s^{-1}\,m)$
<-45 -30 -20 -15 -10 -5 -2 0 0.5 1 1.5 2 2.5 3 >4
$\frac{\partial \alpha}{\partial LAI}(10^{-3} \text{ unitless})$
<-150 -90 -60 -35 -20 -10 -5 0 5 10 20 35 60 90 >150
$\frac{\partial r_a}{\partial LAI}(s\,m^{-1})$
$\frac{\partial r_s}{\partial LAI}(s\,m^{-1})$

Fig. S4. Patterns for each term in Eq. 1 based on CLM5 outputs. (**A-C**) Maps of $\left(\frac{\partial T_s}{\partial \alpha}\right)\left(\frac{\partial \alpha}{\partial LAI}\right)$, $\left(\frac{\partial T_s}{\partial r_a}\right)\left(\frac{\partial r_a}{\partial LAI}\right)$ and $\left(\frac{\partial T_s}{\partial r_s}\right)\left(\frac{\partial r_s}{\partial LAI}\right)$, respectively. (**D-E**) Maps of sensitivities of LST to biophysical factors, that is, $\frac{\partial T_s}{\partial \alpha}$, $\frac{\partial T_s}{\partial r_a}$ and $\frac{\partial T_s}{\partial r_s}$. (**G-I**) Maps of sensitivities of biophysical factors to LAI, that is, $\frac{\partial \alpha}{\partial LAI}$, $\frac{\partial r_a}{\partial LAI}$ and $\frac{\partial r_s}{\partial LAI}$.

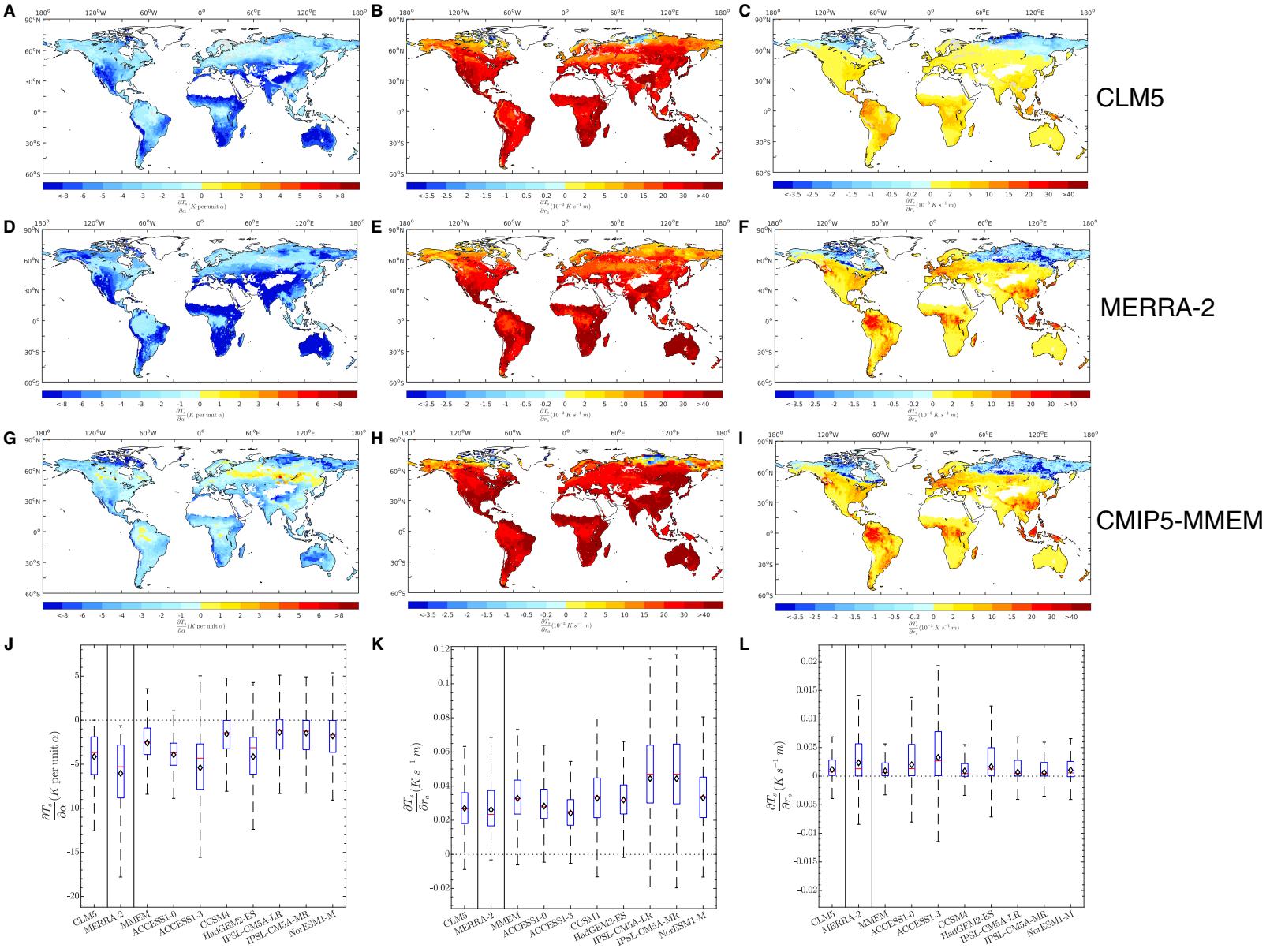
A
B
C
D
E
F
G
H
I
J
K
L
CLM5
MERRA-2
CMIP5-MMEM
CLM5
MERRA-2
MMEM
ACCESS1-0
ACCESS1-3
CCSM4
HadGEM2-ES
IPSL-CM5A-LR
IPSL-CM5A-MR
NorESM1-M

Fig. S5. Sensitivities of LST to biophysical factors in Eq. 1 diagnosed by the TRM method from different inputs. (**A-C**) Maps for $\frac{\partial T_s}{\partial \alpha}$, $\frac{\partial T_s}{\partial r_a}$, $\frac{\partial T_s}{\partial r_s}$ from CLM5. (**D-F**) Similar to (A-C) but from MERRA-2. (**G-I**) Similar to (A-C) but from CMIP5 MMEM. (**J-L**) Boxplot for $\frac{\partial T_s}{\partial \alpha}$, $\frac{\partial T_s}{\partial r_a}$, $\frac{\partial T_s}{\partial r_s}$ from different inputs. CLM5 and MERRA-2 data are from 2000 to 2014, and the CMIP5 data are from 2000 to 2005.

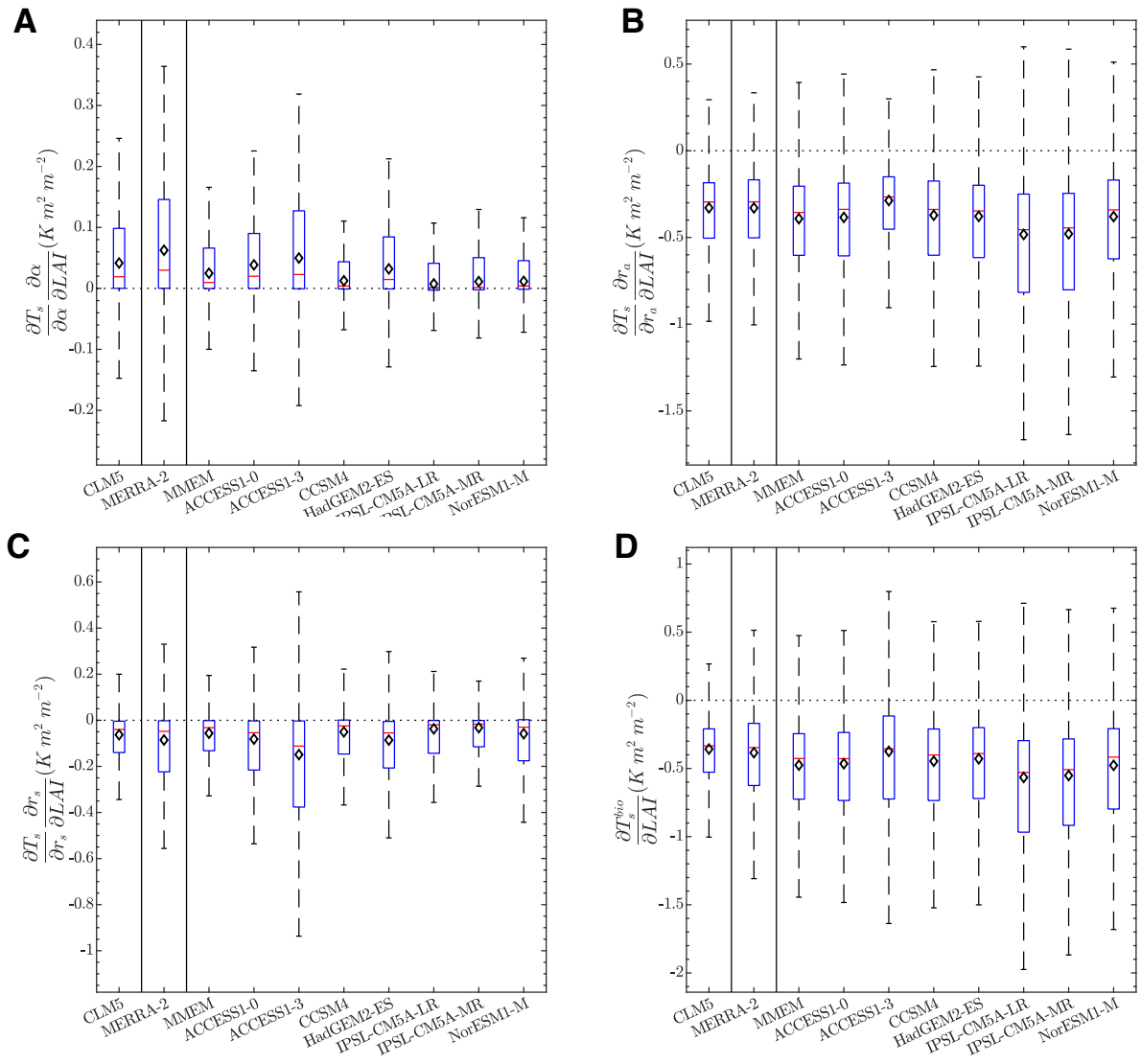

Fig. S6. Boxplot for sensitivities of LST to LAI from different data and models. (**A-C**) $\left(\frac{\partial T_S}{\partial \alpha}\right)\left(\frac{\partial \alpha}{\partial LAI}\right)$, $\left(\frac{\partial T_S}{\partial r_a}\right)\left(\frac{\partial r_a}{\partial LAI}\right)$ and $\left(\frac{\partial T_S}{\partial r_s}\right)\left(\frac{\partial r_s}{\partial LAI}\right)$, respectively. (**D**), $\frac{\partial T_S^{bio}}{\partial LAI}$. Note that the x-axis shows the data sources for sensitivities of LST to biophysical factors, while all sensitivities of biophysical factors to LAI are estimated from CLM5 outputs.

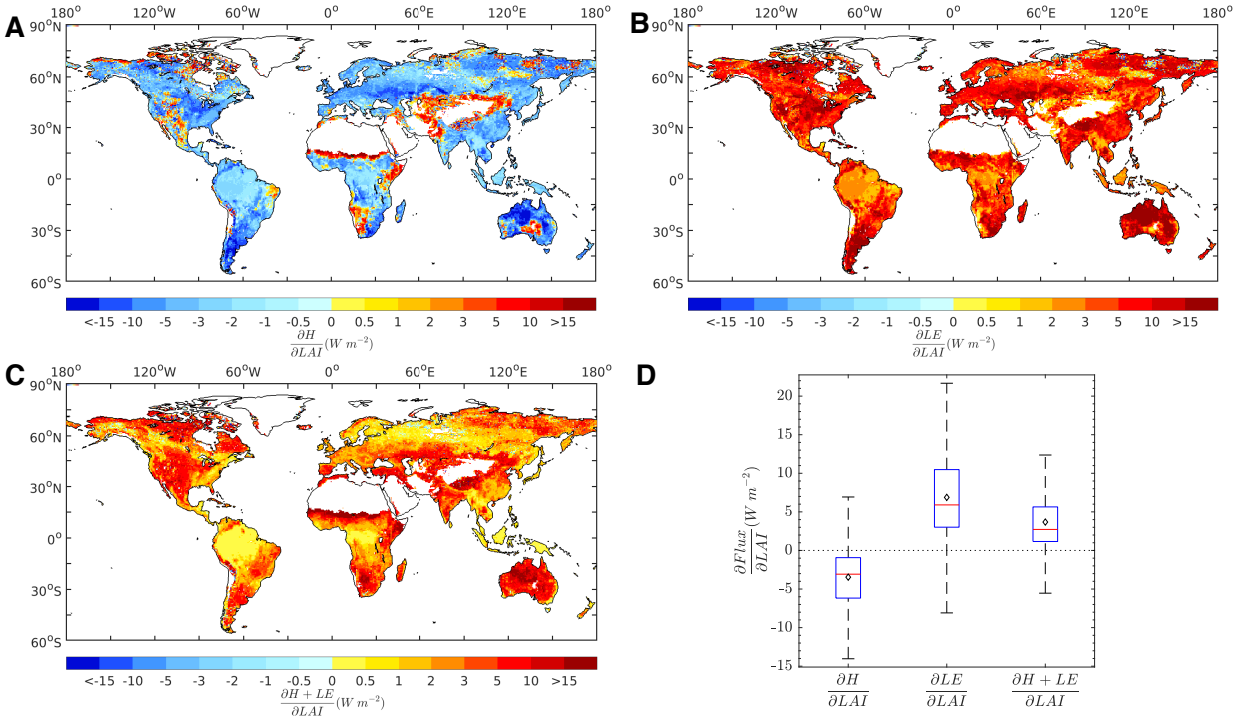

Fig. S7. Sensitivities of sensible and latent heat fluxes to LAI. (**A**), Map for the sensitivity of sensible heat flux to LAI, $\frac{\partial H}{\partial LAI}$. (**B**), Map for the sensitivity of latent heat flux to LAI, $\frac{\partial LE}{\partial LAI}$. (**C**), Map for the sensitivity of available energy to LAI, $\frac{\partial H+LE}{\partial LAI}$. (**D**) Boxplot.

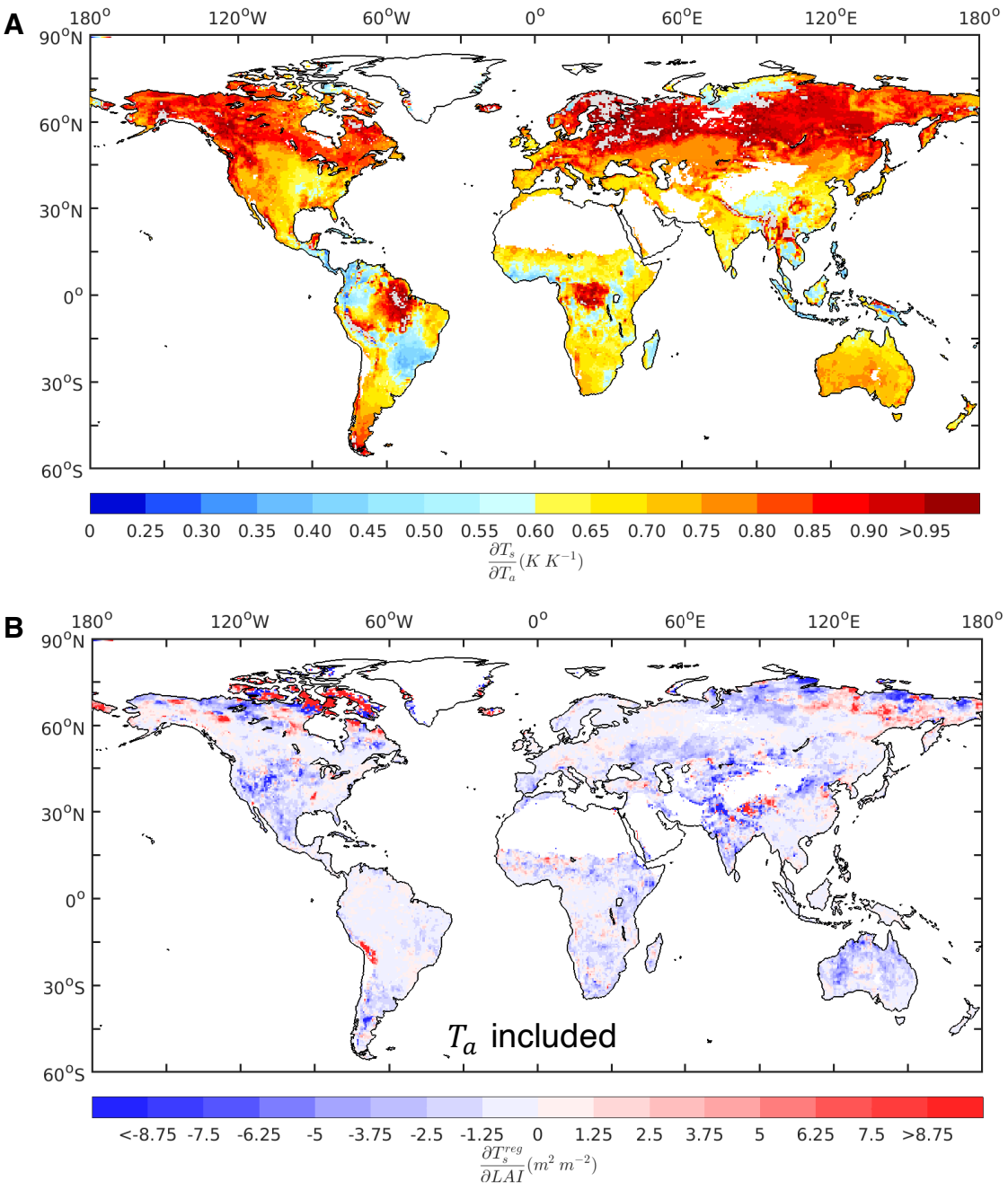

Fig. S8. Sensitivity of LST to air temperature and regressed sensitivity of LST to LAI with air temperature. (**A**) Sensitivity of LST to air temperature at reference height (~30 m) diagnosed by the TRM method and based on CLM5 historical-LAI run outputs. (**B**) Sensitivity of T_s to LAI estimated by the multiple linear regression method using CLM5 outputs with the interannual variability of air temperature included.

Table S1. List of symbols and acronyms.

Symbols	Definitions	Units
α	Albedo	–
r_a	Aerodynamic resistance	s m^{-1}
r_s	Surface resistance	s m^{-1}
ε	Emissivity	–
G	Ground heat flux	W m^{-2}
T_s	Land surface temperature	K
$\frac{\partial T_s}{\partial \alpha}$	Sensitivity of land surface temeperature to albedo	K
$\frac{\partial T_s}{\partial r_a}$	Sensitivity of land surface temeperature to aerodynamic resistance	K s^{-1} m
$\frac{\partial T_s}{\partial r_s}$	Sensitivity of land surface temeperature to surface resistance	K s^{-1} m
$\frac{\partial T_s}{\partial \varepsilon}$	Sensitivity of land surface temeperature to emissivity	K
$\frac{\partial T_s}{\partial G}$	Sensitivity of land surface temeperature to ground heat flux	K W^{-1} m^2
$\frac{\partial \alpha}{\partial LAI}$	Sensitivity of albedo to leaf area index	–
$\frac{\partial r_a}{\partial LAI}$	Sensitivity of aerodynamic resistance to leaf area index	s m^{-1}
$\frac{\partial r_s}{\partial LAI}$	Sensitivity of surface resistance to leaf area index	s m^{-1}
$\frac{\partial \varepsilon}{\partial LAI}$	Sensitivity of emissivity to leaf area index	–
$\frac{\partial G}{\partial LAI}$	Sensitivity of ground heat flux to leaf area index	W m^{-2}
$\Delta T_s^{bio,LAI}$	Change of land surface temeparture due to leaf area index change through biophysical pathways	K m^2 m^{-2}
$\frac{\partial T_s^{bio}}{\partial LAI}$	Sensitivity of land surface temperature to leaf area index through biophysical pathways based on the TRM method	K m^2 m^{-2}
$\frac{\Delta T_s}{\Delta LAI}$	Sensitivity of land surface temperature to leaf area index calculated by CLM5 control and sensitivitity runs	K m^2 m^{-2}
$\frac{\partial T_s^{reg}}{\partial LAI}$	Sensitivity of land surface temperature to leaf area index calculated by multiple linear regression	K m^2 m^{-2}

ΔLAI_{sat}	Change of leaf area index derived from satellite trends	$m^2\ m^{-2}$
$T_{s,sen}$	Land surface temperature in CLM5 sensitivity run	K
$T_{s,ctl}$	Land surface temperature in CLM5 control run	K
LAI_{sen}	LAI in CLM5 sensitivity run	$m^2\ m^{-2}$
LAI_{ctl}	LAI in CLM5 control run	$m^2\ m^{-2}$
α_{sen}	Albedo in CLM5 sensitivity run	–
α_{ctl}	Albedo in CLM5 control run	–
R_n	Net radiation	$W\ m^{-2}$
S_{in}	Incoming shortwave radiation	$W\ m^{-2}$
L_{in}	Incoming longwave radiation	$W\ m^{-2}$
H	Sensible heat flux	$W\ m^{-2}$
LE	Latent heat flux	$W\ m^{-2}$
σ	Stefan-Boltzmann constant	$W\ m^{-2}\ K^{-4}$
ρ	Air density	$kg\ m^{-3}$
c_p	Specific heat of air at constant pressure	$J\ kg^{-1}\ K^{-1}$
L_v	Latent heat of vaporization	$J\ kg^{-1}$
T_a	Air potential temperature	K
q_a	Air specific humidity	$kg\ kg^{-1}$
e^*	Saturation vapor pressure	Pa
P	Atmospheric pressure at the surface	Pa
Q	The equivalent energy of $\Delta T_s^{bio,LAI}$	J
Acronyms	**Definitions**	**Units**

LST	Land Surface Temperature	K
LAI	Leaf Area Index	$m^2\ m^{-2}$
TRM	Two Resistance Mechanism	–
CLM5	Community Land Model Version 5	–
CMIP5	Coupled Model Intercomparison Project 5	–
OWV	Other Woody Vegetation	–
MERRA-2	Modern-Era Retrospective analysis for Research and Applications, Version 2	–
fPAR	Fraction of absorbed Photosynthetically Active Radiation	–
CO_2	Carbon Dioxide	–
CESM2	Community Earth System Model, Version 2	–
GSWP3	The Third Phase of the Global Soil Wetness Project	–
MODIS	Moderate Resolution Imaging Spectroradiometer	–
PFT	Plant Functional Type	–
UCAR	University Corporation for Atmospheric Research	–
AVHRR	Advanced Very-High-Resolution Radiometer	–
IGBP	International Geosphere-Biosphere Programme	–

Table S2. Areal fraction of dominate factors from different models and data.

Unit (%)	CLM5	MERRA-2	MMEM	ACCESS1-0	ACCESS1-3	CCSM4	HadGEM2-ES	IPSL-CM5A-LR	IPSL-CM5A-MR	NorESM1-M
α dominant	3.61	5.97	1.22	1.67	8.19	1.54	4.03	1.28	1.56	1.21
r_a dominant	81.64	67.56	83.81	72.87	51.01	78.65	72.00	84.64	85.57	75.11
r_s dominant	14.74	26.48	14.97	25.45	40.8	19.81	23.97	14.08	12.87	23.68